Sains Malaysiana 46(4)(2017): 637–644
http://dx.doi.org/10.17576/jsm-2017-4604-017

Bifunctional Regenerated Cellulose Membrane Containing TiO_2 Nanoparticles for Absorption and Photocatalytic Decomposition

(Dwifungsi Membran Selulosa yang Terjana Semula dengan Kandungan TiO_2 untuk Proses Penyerapan dan Penguraian secara Fotopemangkinan)

EVYAN YANG CHIA YAN, SARANI ZAKARIA*, CHIN HUA CHIA & THOMAS ROSENAU

ABSTRACT

A simple and green method was presented to embed TiO_2 on regenerated cellulose membranes via cellulose dissolution-regeneration process. The physical, chemical and mechanical properties of the composite membranes were characterized by X-ray diffraction (XRD), scanning electron microscopy (SEM), Fourier- Transform Infrared (FTIR), ultraviolet (UV) - visible spectroscopy and tensile test. The results indicated that cotton linter has been converted from cellulose I to cellulose II after the regeneration process, while the TiO_2 nanoparticles embedded inside the membrane maintaining its original crystal structures. The TiO_2 composite membranes possessed high ability of water absorption with total pore volume ranged from 0.45±0.01 to 0.53±0.02 cm^3/g. The elongation at break of the prepared membranes increased 29% averagely from dry state to wet state. The tensile strength of the membranes remained at a minimum value of 0.50±0.03 MPa in wet state thus enabled the films to withstand in wet for long period of time under weak UV irradiation. The regenerated cellulose membranes with TiO_2 performed well in photocatalytic activity while exhibiting distinct absorption abilities. This study provides a potential application in energy-saving decomposition system in which the dye compound can be easily removed via two simultaneous pathways: Absorption and photocatalytic decomposition.

Keywords: Absorption; mechanical properties; photocatalysis; regenerated celloluse

ABSTRAK

Kaedah yang mudah telah dikemukakan untuk menerap TiO_2 pada membran selulosa yang diperbaharui melalui proses pelarutan-penjanaan semula selulosa. XRD, SEM, FTIR, Spektroskopi UV - Vis dan mesin ujian tegangan digunakan untuk mencirikan sifat fizikal, kimia dan mekanik membran komposit. Hasil analisis menunjukkan linter kapas telah berubah daripada selulosa I kepada selulosa II selepas proses penjanaan semula. Manakala, TiO_2 yang bertabur dalam membran mengekalkan struktur kristalnya. Membran komposit TiO_2 yang dihasilkan memiliki keupayaan penyerapan air yang tinggi dengan jumlah liang dari 0.45±0.01-0.53±0.02 cm^3/g. Keseluruhannya, pemanjangan membran kering meningkat sebanyak 29% berbanding dengan membran dalam keadaan basah. Membran yang dihasilkan dapat mengekalkan kekuatan tegangan pada nilai minimum 0.05±0.03 MPa dalam keadaan basah untuk tempoh yang panjang di bawah sinaran UV yang lemah. Membran selulosa berkandungan TiO_2 menunjukkan prestasi yang baik dalam aktiviti foto-pemangkinan sementara mempamerkan keupayaan penyerapan. Kajian ini berpotensi diaplikasikan dalam sistem penguraian dengan menjimatkan kos dan tenaga. Sebatian boleh diuraikan dengan mudah melalui dua cara serentak: penjerapan dan penguraian secara foto-pemangkinan.

Kata kunci: Foto-pemangkinan; membran terjana semula; penyerapan; sifat mekanik

INTRODUCTION

Rapid development in industry has accelerated the production and accumulation of by-product wastes which have resulted in severe environmental pollution. Water pollution is one of the major concerns since it is much related to mankind survival. Recently, the most effective and attractive water treatment method is advanced oxidation process (AOP). AOP is innovative and environmental friendly especially for water treatment which driven by suitable light source depending on the type of catalyst (Leong et al. 2014). Unlike the conventional water treatment, hydroxyl radicals are generated in the presence of photons during the catalysis process. These hydroxyl radicals are the strongest oxidant after fluorine in aqueous solution. They play important roles in the degradation of toxic organic compounds and into simple and safe inorganic molecules without appearance of secondary waste (Mital & Manoj 2011). There are various semiconductor materials that have been investigated as photocatalysts in AOP or known as heterogeneous photocatalytic oxidation, e.g. ZnO (Liu et al. 2013; Wan et al. 2015), Fe_2O_3 (Lee et al. 2014) and WO_3 (Hernandez-Uresti et al. 2014). TiO_2 is one of the benchmarks for photocatalytic performance because they are photo-stable and chemical-stable in solution, availability, non-hazardous for humans and eco-environment (Ruslime et al. 2011).

Among three phases of TiO_2: Anatase, rutile and brookite, anatase and rutile are desired to be used as photocatalyst under irradiation of light with wavelength, 250 nm < λ n < 380 nm, namely in the range of UV light. A redox condition to approaches upon the UV light radiation as the photons (*h*) with energy equal or greater than the band gap energy (E_g). This results in excitation of electrons at valence band to become negative electron (e^-) at the conduction band and generation of positive holes (h^+) at valence band. E_g is the difference of energy between the filled valance band and the empty conduction band, E_g for TiO_2 - anatase is 3.2eV and E_g for TiO_2 - rutile is 3.0 eV (Teh et al. 2011). The photogenerated e^- and h^+ pair can either recombine or participate in the redox reaction. The non- recombined e^- and h^+ pair will migrate to the surface of TiO_2 to take part in the redox reaction as below (Leong et al. 2014):

$$\text{For electron, } Ti(IV) + \bar{e} \rightarrow Ti(III), \quad (1)$$

$$Ti(III) + O_2 \rightarrow Ti(IV) + O_2^{\bullet -}, \quad (2)$$

$$R + O_2^{\bullet -} \rightarrow\rightarrow \text{intermediates} \rightarrow\rightarrow H_2O + CO_2, \quad (3)$$

$$\text{For holes instantly, } H_2O + h^+ \rightarrow OH^{\bullet} + H^+, \quad (4)$$

$$R + OH^{\bullet} \rightarrow\rightarrow \text{intermediates} \rightarrow\rightarrow H_2O + CO_2. \quad (5)$$

The superoxide reactive radicals, $O_2^{\bullet -}$ and hydroxyl radicals, $OH^{\bullet}$ can oxidize organic reactant (R) as in (3) and (5). Some of the viruses, bacteria and microorganisms can also be inactivated by them (Rahim et al. 2012).

It is necessary to prepare a system which is able to separate the nano-sized TiO_2 with the treated aqueous system. The ordinary hosts of the nanoparticles that have been used include ceramic, glass, polymer and fibres. Based on literature, the electrical, magnetic and optical properties of the inorganic nanoparticles can be retained in polymer matrix (Chook et al. 2015; Zhu et al. 2012). This has promoted the idea to create an inorganic nanoparticle/ polymer composite as effective catalyst.

Nowadays, the remarkable properties of cellulose, such as abundance, biodegradable and environmental friendliness, has established itself a useful renewable resource. Regenerated cellulose (RC) membrane has been proven to be stable under UV exposure as well as in oxidative environment (Djafer et al. 2010). In addition, the RC film possesses porous structure and high absorption ability. This is one of the surface functionality with hydroxyl group (Cai et al. 2007) leading to its important characteristics in water treatment system in order to absorb more pollutant and undergo photodegradation. On top of that, the organic-inorganic hybrid cellulose nanocomposites have attracted researchers due to their outstanding properties to be applied widely in various fields including biomedicine, food packaging and water purification. In current study, cotton linter as cellulose base went through regeneration process to fabricate RC membranes in order to suspend TiO_2 powder onto them. These TiO_2 composite regenerated (TRC) membranes behaved as photocatalytic membrane reactor where the photocatalytic decomposition can proceed under stable condition and be easily removed after usage. The photocatalytic mechanism of the membrane is schematized in Figure 1.

Materials and Methods

Materials

Commercial titanium dioxide powder with an average particle size of 21±5 nm, was purchased from Sigma Aldrich. The cotton linter with average molecular weight, M_η of 9×10^4 was obtained from Hubei Chemical Fiber Co. Ltd., China. All other chemical regents, such as lithium hydroxide (LiOH, 98%), urea (CH_4N_2O, 99%) and sulphuric acids (H_2SO_4, 98%) were of analytic grade and purchased from Sigma Aldrich. All chemicals were used without further purification.

Experimental Procedures

Preparation of Regenerated Cellulose (RC) Membrane

The production of regenerated cellulose membrane was modified from Kaco's research group (Kaco et al. 2014) as reported earlier; an aqueous solution of LiOH/urea solution was prepared with weight ratio of 4.6:15. The aqueous solution left to freeze in the freezer for at least 8 h. 3.5 wt. % of cotton linter was then rapidly dissolved in the LiOH/urea solution under vigorous stirring. A transparent cellulose solution known as cellulose solvent was produced after approximately 5 min of stirring. The obtained cellulose solution was subjected to centrifugation at 5°C for 10 min to remove air bubbles. The soluble cellulose solution casted on a glass plate to form a thin layer of membrane and immersed into an aqueous coagulating bath containing 5 wt. % Na_2SO_4 to regenerate the cellulose. The formed membrane was washed with deionized water to remove the excessive chemical.

Preparation of RC/TiO_2 (TRC) Membrane

For preparation of TiO_2 embedded in cellulose membranes (TRC), various weight ratios of TiO_2: cellulose were set. A desired amount of the commercial TiO_2 powder was dispersed into deionized water under sonication. The TiO_2 solution then added into the LiOH/urea aqueous solution which was the same as described for the preparation of plain regenerated cellulose membrane. The produced membranes were freeze-dried using Freeze Dryer (Scanvac Cool Safe -110-4) for 48 h before the characterization. The prepared TRC membranes were labelled according to the weight ratio of TiO_2: cellulose for 1:7 as TRC1, 3:7 as TRC2, 5:7 as TRC3 and 7:7 as TRC4 meanwhile plain regenerated membrane without TiO_2 was labelled as RC.

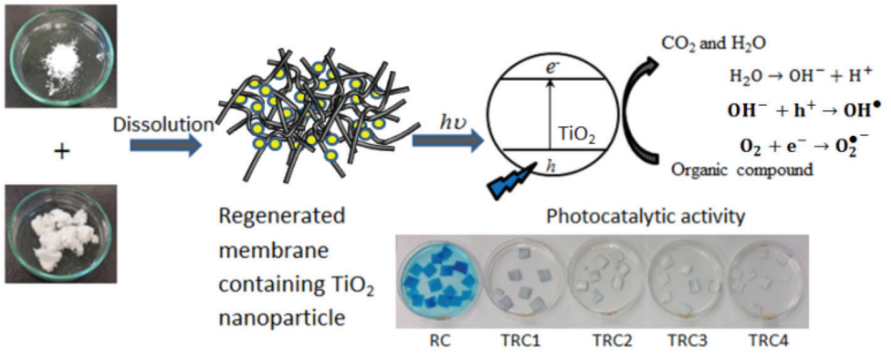

FIGURE 1. Schematic diagram of the production and photocatalytic activity of regenerated cellulose membranes containing TiO_2

CHARACTERIZATION

The freeze-dried membranes and TiO_2 powder were analysed using X-ray Diffractometer (XRD, Bruker AXS D8 Advance) with Cu-K_α radiation from the range of 6° to 80°. The field emission scanning electron microscope (FESEM) images were obtained from FESEM Zeiss/Supra 55VP for morphology observation. The Raman measurement was performed on a Fourier transform infrared spectroscopy spectrometer (ATR-Perkin Elmer Spectrum 400 FT-IR).

WATER ABSORPTION MEASUREMENT

The method and condition of water absorption test was conducted according to the standard of ASTM D570-98. The freeze-dried membranes were cut into 7.6 × 2.5 cm with thicknesses approximately 1 mm. The variation of thickness for each was ±0.2 mm. The samples were dried again in an oven at 50°C for at least 16 h to remove moisture and kept in a desiccator for 30 min. The samples were weighed variations to the nearest 0.001 g immediately after withdrawal from the oven. The samples were submerged into different beakers filled with 50 mL distilled water accordingly and covered with aluminium foil for 2 and 24 h. The percentage of weight gain (wt. %) during the immersion in distilled water was calculated as in (6) (Mohammad et al. 2014):

$$W\% = \frac{W_{wet} - W_{dry}}{W_{dry}} \times 100\%, \quad (6)$$

where W_{wet} is the weight of sample after immersion into distilled water for 2 or 24 h; and W_{dry} is the weight of sample before immersion into distilled water.

Meanwhile, the pore volumes (V_p) of the samples were calculated through the water uptake of the membranes. Since water did not dissolve cellulose and TiO_2, therefore value of V_p can be determined from (7) (Pojanavaraphan et al. 2011):

$$V_p = \frac{M_{wet} - M_{dry}}{\rho \bullet M_{dry}}, \quad (7)$$

M_{dry} is the mass of sample before immersion into distilled water; M_{wet} is the mass of sample after immersion into distilled water until it reach swelling equilibrium; and ρ is the density of water (0.997g/mL at 25°C).

TENSILE TESTING ON MECHANICAL PROPERTIES

The tensile properties of the membranes were tested using a Universal Testing Machine (Gotech Al-3000) according to ASTM D882-12. The samples were cut into strips with the length of 10 cm, width of 1 cm and average thickness about 1 mm, which was measured from top, middle and bottom of the strips. The load of the testing machine was 10 kgf and the speed of testing was set at 5 mm/min. The values of elastic modulus, tensile strength and elongation were determined from the stress-strain curve that obtained from software analysis of GoTech U62 64 bits (Ver. 20140227-6227). Tensile testing was carried on the same set of samples after immersion in water for at least 24 h under the same condition and remained the setting of the testing machine.

PHOTOCATALYTIC ACTIVITY MEASUREMENT

The dried membranes with different content of TiO_2 were cut into dimension of 1 × 1 cm. 0.1ng of cut membrane were immersed into a petri dish containing 20 mL of methylene blue (MB - 10 mg/L). MB is a heterocyclic aromatic chemical compound ($C_{16}H_{18}CIN_5S$) which was used as dye in the study. It is famous as redox indicator because of its high effectiveness in exhibiting the oxidation reaction in the form of its blue colour disappearance. The submerged samples were left in a chamber to avoid and minimize emission of light on the samples for 24 h to allow the membranes to achieve swelling equilibrium. After 24 h, photocatalytic activity subsequently conducted in the chamber equipped with three TL 8W black light lamps which are positioned on top and both sides of the chamber to be functioned as artificial UV light. The decolouration of MB was analysed using a UV-Vis spectrophotometer (Jenway 7315) to determine the concentration of MB over time. The percentage of degradation of MB ($D\%$) was determined according to (8):

$$D\% = \frac{C_e}{C_o} \times 100\%, \quad (8)$$

C_o is the concentration of MB before photocatalytic activity; C_e is the concentration of MB each hour during photocatalytic activity; and the experiment was run for 6 h and prolonged for 72 h until a complete decolouration achieved.

Results and Discussion

Morphology and Structure of the RC and TRC Membranes

A good catalyst in photocatalytic activity should possess the properties such as high in material purity, porosity and surface area and narrow pore size distribution (Choi et al. 2007). TiO_2 nanoparticle as shown in SEM Figure 2(a) is a commercial TiO_2 powder which is famous for its almost excellent photocatalytic properties. The very small particle size - 21 ± 5 nm (as labelled by Sigma Aldrich) guaranteed it to be high in surface area. The surface morphology of the plain RC membrane is shown in Figure 2(b). The homogenous macroporous structures which were considered as extrinsic porosity had been observed on the membranes under SEM. These porous structures and hydroxyl groups had prepared cavities for inorganic nanoparticles to be entrapped onto them. The –OH groups that formed in the RC membranes promoted hydrophilicity in the surfaces and enhanced the interaction of RC with the surfactants which made TiO_2 easily to be absorbed in to the RC membrane during the coagulation bath. Meanwhile, longer period was required for the exchange between the solvent and non-solvent through the TiO_2 entrapped in RC membrane formation compared to neat RC membrane (Rahimpour et al. 2008). Consequently, more pores were developed in the membrane with higher content of TiO_2 which resulted in dispersion of TiO_2 nanoparticles on the film as exhibited in Figure 2(c) and 2(d). However, higher concentration of TiO_2 in casting solution would result in larger aggregates in the membrane matrix. According to Liu et al. (2010), the aggregation also increases by the ability of polymer membrane that tends to aggregate in parallel to each other. This phenomenon was noticeable on the film which contained with high fraction of TiO_2 as shown in Figure 2(d).

Figure 3 displays the FTIR spectra of raw cotton linter and plain regenerated cellulose (RC) membrane. The peak at 2899.59 cm^{-1} which corresponded to –CH stretching of pure cotton linter was shifted to 2894.13 cm^{-1} after rapid dissolution with LiOH and Urea. The transmittance peak at 1029.61 cm^{-1} due to C-O at C-6 stretching vibration was shifted to 1081.81 cm^{-1} after the regeneration. Meanwhile, the C-O stretching vibration of C-O-C groups was moved from 897.70 to 895.00 cm^{-1}. The stretching vibration of –OH ranged from 3000 to 3700 cm^{-1} for both pure cotton linter and RC membrane, however, the band was broadened on RC membrane. The band characteristics of both raw cotton linter and RC membrane were related to the transition of

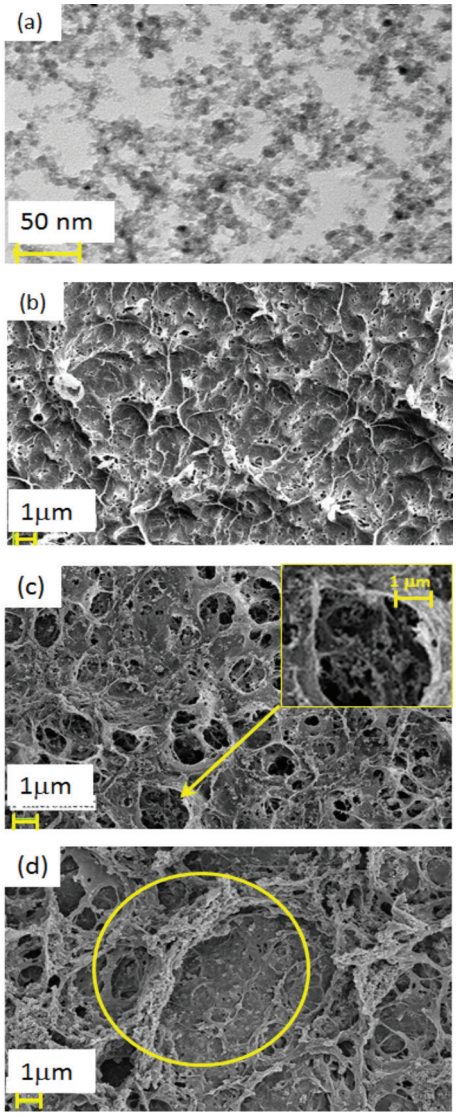

FIGURE 2. (a) TiO_2 nanoparticle, (b) Plain regenerated cellulose membrane, (c) & (d) TiO_2 embedded in regenerated cellulose membranes

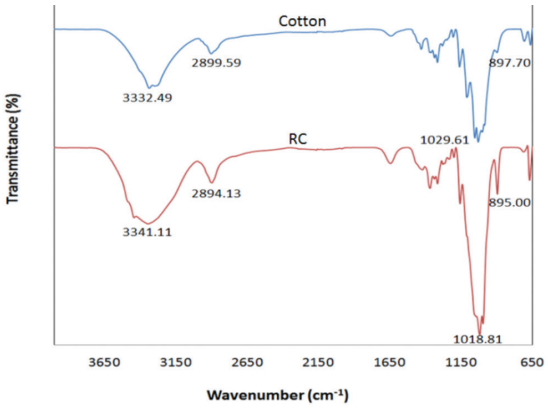

FIGURE 3. FTIR spectra of pure cotton linter and regenerated cellulose (RC) membrane

cellulose I to cellulose II. Transmittance peaks near 2894 cm^{-1} was exhibited by the RC and all the TRC membranes due to the stretching vibration of C-H were remained as shown in Figure 4. Meanwhile, the H-O-H bending from the moisture absorption was characterized by the occurrence of peaks around 1639 cm^{-1} (Zhang et al. 2012). There was drastic decreasing of transmittance in the range of 670 to 895 cm^{-1} and the bands were widened when moving to the lower wavenumber in all the TRC membranes compared to the plain RC membrane spectra. These could be caused by the Ti-O stretching mode in TiO_2 powder which was embedded in cellulose matrix. New peak did not exist for all the TRC membranes and this had proven that the physical interaction played a role in the formation of TRC membranes with no new chemical bonding appeared.

Figure 5 shows the XRD patterns of RC, TRC and TiO_2 powder. The peaks at $2q$ = 12.07°, 20.1° and 21.6° in Figure 5(a) signifies the formation of cellulose II crystalline on the planes of, (110) and (020), respectively. There were sharp peaks as shown in Figure 5(f) with high intensity obviously indicated that TiO_2 is in the phases of anatase (A) and rutile (R) in Figure 5(f). The anatase and rutile phases of TiO_2 were both in tetragonal crystalline structures, thus, they reflected higher intensity of light in the X-ray diffraction compared to cellulose II as displayed in Figure 5(b) - 5(e). This resulted in the peaks of cellulose II could not be evidenced because they superpose with the diffraction lines of TO_2 in the XRD patterns for TRC membranes. There were no significant changes among all the TRC patterns. In addition, this implied that the

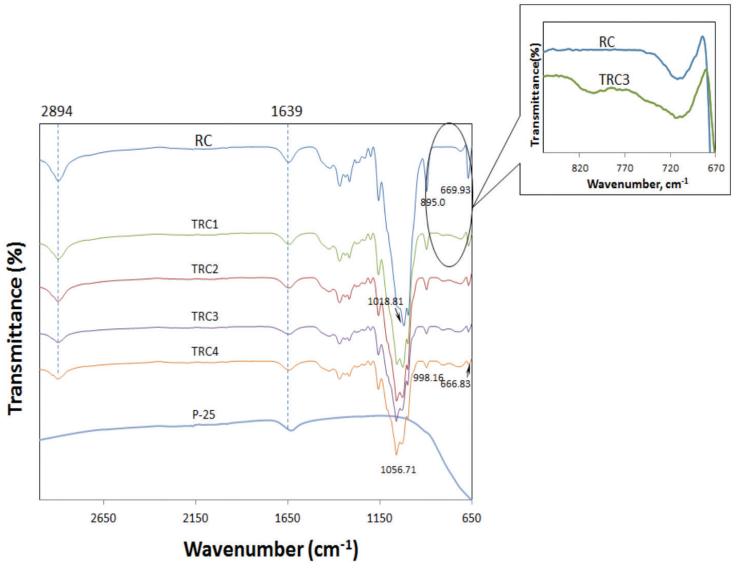

FIGURE. 4. FTIR spectra of plain RC membrane, TiO_2 embedded RC (TRC) membrane and TiO_2 powder

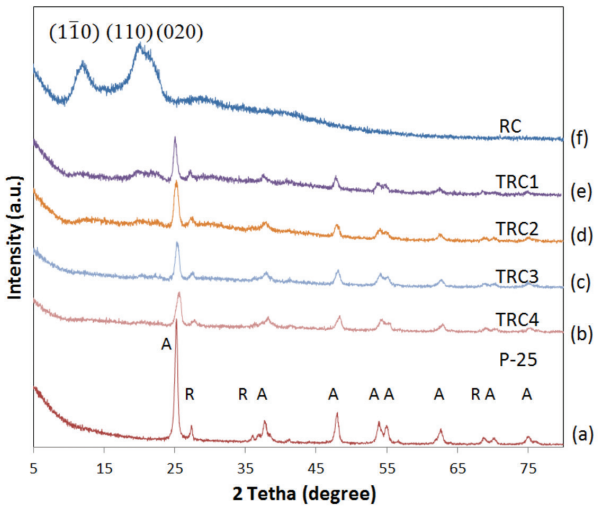

FIGURE 5. XRD patterns of (a) plain RC membrane, (b) - (e) TRC membranes with different ratio of TiO_2: cellulose and pure TiO_2 powder

dissolution of cellulose did not change the crystalline phases of TiO_2. Based on the XRD data, the average crystallite size of TiO_2 before entrapping in RC membrane was 14.5 nm and the estimated average crystallite size of TiO_2 after entrapping in RC membrane was 13.3 nm. From the calculation, it was clearly showed that the crystallite sizes of TiO_2 did not affect as the chemical reaction did not take place between TiO_2 and other chemicals during the regeneration of cellulose. This confirmed with the FTIR results which indicated that new chemical bond did not exist.

WATER ABSORPTION BEHAVIOUR

The plain RC membrane exhibited good absorption ability towards water. Conversely, the ability dropped markedly by increasing TiO_2 contents as shown in the graph of Figure 6 in terms of total pore volume, V_p. The values of V_p decreased from 0.65 to 0.45 cm^3/g with the increasing of weight fraction of TiO_2 - cellulose in TRC membranes. This was attributed to the water uptake resistance of the nanocomposite membranes. The potential of aggregation of nanoparticles could decrease the effective surface of TiO_2 and hence declined the hydroxyl groups on the surface of TRC membranes. The absorption processes were essentially controlled by mass diffusion and particle diffusion as the chemical reaction did not occur between water molecules and RC or TRC film. That is, the greater amount of TiO_2 obstructed the pores of the membranes and reduced the absorption ability as reported by Rahimpour et al. (2008). The absorption of water took place effectively for the first 2 h; however it was prolonged gradually overnight referring to Figure 6. This implied by the hydrophilicity of RC which intrinsically performed at the beginning of the absorption process within 2 h. However, after 2 h, the diffusion of water molecules reduced for all the RC and TRC membranes. This was due to the high absorbance of water molecules onto the films within 2 h in turn to create weak attraction on the surface which was caused by the surface tension of water molecules. Therefore, the moisture uptake of the films after 2 h has slowed down. The plain RC membrane continued about 14.5% absorption within 24 h whereas the TRC membranes only extended the water absorption from 3 to 5% (bar chart of Figure 6). This was corresponded to the much lower hydrophilicity property of TiO_2 compared to the pure RC membrane. Therefore, RC loaded with higher content of TiO_2, the absorption ability would be lower as TiO_2 nanoparticles dispersed inhomogenously in the RC membranes (Mohammad et al. 2014) and resulted in increasing of total solid content. The data was in good agreement with the scheming of V_p (graph of Figure 6) which reflected that the TiO_2 loading lowered the absorption capacity of the membrane. There was no further change in weight after 24 h submerging in water which obviously indicated that saturation had been achieved.

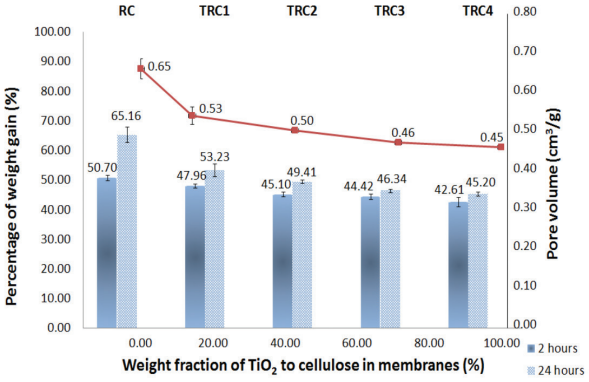

FIGURE 6. Total pore volumes and percentage of weight gain for RC and TRC with different weight fraction of TiO_2 to cellulose

MECHANICAL PROPERTIES

The mechanical properties of pure RC and TRC membranes were investigated to determine the effects of TiO_2 incorporation. According to Table 1, the tensile strength (σ) and elongation at break (ε) of the RC membrane decreased moderately as the adding of TiO_2 content increased in both dry and wet state. This was mostly because TiO_2 nanoparticles affected the final structures of RC during the formation of the membrane. Some of the TiO_2 particles dispersed inhomogenously and aggregated intensely in the composite membranes as shown in Figure 2(d) as discussed in previous section. Therefore, this resulted in the tensile strength dropped corresponding to the addition of TiO_2 contents. On the other hand, the values of σ in wet state increased drastically which consequently gave arise to high ductility if compared with those in dry state. The high water permeability was the main factor of the increasing of ductility. RC membranes possessed high V_p as mentioned earlier. When more water molecules had been entrapped on the membrane during immersion in the water, the weak attraction between water molecules and the membrane structures would be enhanced and thus resulted in improvement of ductility. However, the values of σ dropped when the membranes tested in wet state compared to dry state. In this case, the high content of water weakened the values of σ for the wet membranes, they were not able to withstand high stress. Although the values of σ was dropped in wet state, the strength values ranged from 0.50±0.03 to 0.87±0.06 MPa was strong enough to let the membrane sustained in wet state for a long period of time (>24 h). The RC and TRC membrane did not perform elastic modulus in wet state since they were low in elasticity which was caused by the water molecules that situated in the pores of the membranes. Therefore, they could not return to their original dimension as the load had been removed. Meanwhile, the results were delighted with very high elastic modulus (1.96 - 3.47GPa) for TRC membranes in dry state. The mechanical properties that well performed by the prepared TRC membranes could be recommended for a promising practical application either in wet state or dry state.

TABLE 1. Tensile strength and elongation of membranes before and after water absorption

Material	Wet state		Dry state		
	Tensile strength, σ (MPa)	Elongation at break, ε (%)	Elastic modulus (GPa)	Tensile strength, σ (MPa)	Elongation at break, ε (%)
RC	1.04±0.10	70.89±0.84	4.07±0.25	70.10±1.34	8.17±0.25
TRC1	0.87±0.06	37.49±0.79	3.47±0.30	36.13±1.33	2.93±0.30
TRC2	0.71±0.03	34.86±1.13	2.93±0.13	31.60±1.30	2.85±0.13
TRC3	0.66±0.03	32.62±1.26	2.16±0.20	25.48±0.66	2.42±0.20
TRC4	0.50±0.03	20.72±1.42	1.96±0.15	13.59±0.86	1.77±0.15

PHOTO-REACTIVITY PERFORMANCE

The direct excitation of TiO_2 which is a semiconductor occurs according to the following reactions:

$$TiO_2 + \text{UV light} \rightarrow h^+ + e^- \quad (9)$$

As explained earlier, the e^- will reduce Ti(IV) to Ti(III) (1) and consequently react with the absorbed oxygen on the surface of TiO_2 to superoxide radical anions ($O_2^{\bullet-}$) meanwhile TiO_2 nanoparticles played an important role in photocatalytic activities hence the photodegradation of the TRC membranes with the highest weight fraction of TiO_2 (TRC4) displayed the most effective photocatalytic activity. However, it was interesting to note that the photo-degradation of all TRC membrane showed nearly the same pattern after 20 h from Figure 7(b). This could be due to the aggregation that formed on the membranes after long UV irradiation which reduced the photocatalytic activities, especially for the membranes with high TiO_2 content. However, the absorption ability of the cellulose membranes seemed to take over the role of photocatalytic activities gradually after long period of time (>20 h). This was due to the radicals formed by the excitation under UV illumination would oxidize the closest MB molecules which had been fully absorbed onto the films followed the reactions in (3) and (5). In this case, the higher the values of V_p (Figure 6) in TRC membranes, the more pores were accessible for absorption of MB molecules. Therefore this permitted photocatalytic activities executed effectively even though the presence of TiO_2 content was low. The degradation involved the conversion of organic carbon into harmless gaseous CO_2. Meanwhile, those of nitrogen and sulfur heteroatoms from the heterocyclic aromatic MB convert into inorganic ions such as nitrate, ammonium and sulfate ions according to Houas et al. (2001). However, the oxidation process plays the most important role for the disappearance of MB's major part as reported by most of the researchers. This could be explained based on the opening of aromatic rings with the transient formation of carboxylic acids after the evolution of CO_2 according to the 'photo-Kolbe' reaction (Houas et al. 2001):

$$R\text{–}COO^- + h^+ \rightarrow R^{\bullet} + CO_2$$

The 'photo-Kolbe' reaction prompted the removal colour of MB gradually. Nevertheless, the concentration of MB solution in RC plain membrane showed slightly upsurge which might be caused by contamination after longer period of time and this has clearly shown the advantage of TiO_2 for its self-cleaning properties to avoid further contamination from the air. All the TRC film achieved 100% degradation after three days under UV irradiation.

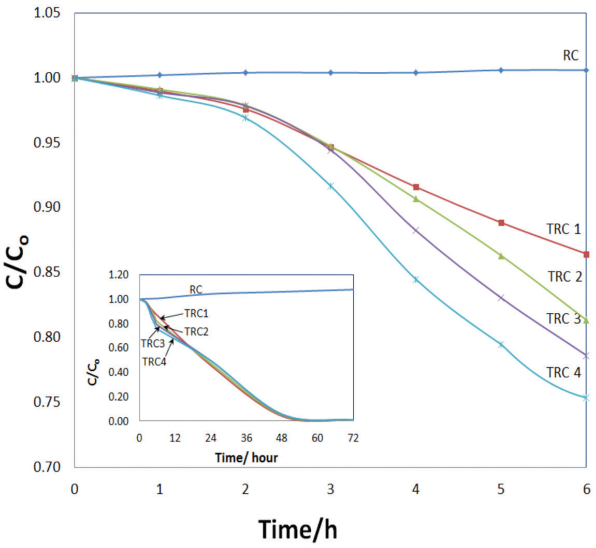

FIGURE 7. (a) The photocatalytic degradation of RC and TRC membranes for 6 h, (b) the photocatalytic activity prolonged for 72 h

CONCLUSION

TiO_2 nanoparticles were successfully incorporated into regenerated cellulose (cotton linter) to form membrane using easy and low cost dissolution-regeneration method. The crystal structure of cellulose were transformed from cellulose I to cellulose II while maintaining the nanocrystalline structure of TiO_2. The prepared membranes exhibited high absorption abilities and stable mechanical properties. The finding gave a suggestion on i.e. long period (>24 h) decomposition system under weak UV irradiation. The photocatalytic decomposition conducted using this portable membrane was based on its bifunctional properties: Absorption and photo-degradation simultaneously. The system could be designed with minimum observation and low consumption of TiO_2 as the cost-saving factor.

ACKNOWLEDGEMENTS

The authors appreciate supports from the grants of LRGS (TD/2012/USM-UKM/PT/04), AP (2015-005), PRGS (1/13/SG07/UKM/01/1), Nilai University Research Grant (MS006) and the Ministry of Higher Education, Malaysia for MyBrain 15-MyPhD scholarship. The authors also thank the Centre for Research and Instrumentation Management (CRIM) at Universiti Kebangsaan Malaysia (UKM) for providing the XRD, FESEM and FTIR testing.

REFERENCES

Cai, J., Zhang, L., Zhou, J., Qi, H., Chen, H. Kondo, T., Chen, X. & Chu, B. 2007. Multifilament fibers based on dissolution of cellulose in NaOH/urea aqueous solution: Structure and properties. *Advanced Materials* 19(6): 821-825.

Choi, H., Stathtos, E. & Dionysiou, D.D. 2007. Photocatalytic TiO_2 film and membranes for the development of efficient wastewater treatment and reuse system. *Desalination* 202: 199-206.

Chook, S.W., Chia, C.H., Zakaria, S., Ayob, M.K., Huang, N.M., Neoh, H.M. & Jamal, R. 2015. Antibacterial hybrid cellulose-graphene oxide nanocomposite immobilized with silver nanoparticles. *RSC Advances* 33: 26263-26268.

Djafer, I., Ayral, A. & Ouagued, A. 2010. Robust synthesis and performance of a titania-based ultrafiltration membrane with photocatalytic properties. *Separation and Purification Technology* 75: 198-203.

Hernandez-Uresti, D.B., Sánchez-Martínez, D., Martínez-de la Cruz, A., Sepúlveda-Guzmán, S. & Torres-Martínez, L.M. 2014. Characterization and photocatalytic properties of hexagonal and monoclinic WO_3 prepared via microwave-assisted hydrothermal synthesis. *Ceramic International* 40(3): 4767-4775.

Houas, A., Lachheb, H., Ksibi, M., Elaloui, E., Guillard, C. & Herrmann, J-M. 2001. Photocatalytic degradation pathway of methylene blue in water. *Applied Catalysis B: Environmental* 31: 145-157.

Kaco, H., Zakaria, S., Razali, N.F., Chia, C.H., Zhang, L. & Jani, S.M. 2014. Properties of cellulose hydrogel from kenaf core prepared via pre-cooled dissolving method. *Sains Malaysiana* 43(8): 1221-1229.

Lee, K.M., Abdul, H.A., Mohd, Z.H. & Zulkarnain. 2014. Synthesis and photocatalysis of ZnO/γ-Fe2O3 nanocomposite in degrading herbicide 2,4-dichlorophenoxyacetic acid. *Sains Malaysiana* 43(3): 437-441.

Leong, S., Razmjou, A., Wang, K., Hapgood, K., Zhang, X. & Wang, H. 2014. TiO_2 based photocatalytic membrane: A review. *Journal of Membrane Science* 472: 167-184.

Liu, H.Y., Liu, D.G., Yao, F. & Wu, Q.L. 2010. Fabrication and properties of transparent polymethymethacrylate/cellulose nanocrystal composites. *BioTechnology* 101: 5685- 5692.

Liu, S., Wang, X., Zhao, W., Wang, K., Sang, H. & He, Z. 2013. Synthesis, characterization and enhanced photocatalytic performance of Ag_2S-cuopled ZnO/ZnS core/shell nanorods. *Journal Alloys Compound* 568: 84-91.

Mital, G.S. & Manoj, T. 2011. A review of TiO_2 nanoparticles. *Chinese Science Bulletin* 56: 1639-1657.

Mohammad, S., Mat, U.W., Wong, T.W., Noel, I.A., Raheleh, H.P. & Abdirahman, A.Y. 2014. Bionanocomposite of regenerated cellulose/zeolite prepared using environmentally benign ionic liquid solvent. *Carbohydrate Polymer* 106: 326-334.

Pojanavaraphan, T., Liu, L., Ceylan, D., Okay, O., Magaraphan, R. & Schiraldi, D.A. 2011. Cellulose cross-link natural rubber (NR)/clay aerogel composite. *Macromolecules* 44: 923-931. DOI 10.1021/ma102443k.

Rahim, S., Radiman, S. & Hamzah, A. 2012. Inactivation of *Escherichia coli* under flourescent lamp using TiO2 nanoparticles synthesized via sol gel method. *Sains Malaysiana* 41(2): 219-224.

Rahimpour, A., Madaeni, S.S., Taheri, A.H. & Mansourpanah, Y. 2008. Coupling TiO_2 nanoparticles with UV irradiation for modification of polyethersulfone ultra-filtration membranes. *Journal of Membrane Science* 313: 158-169.

Ruslime, C.A., Razali, H. & Khairul, W.M. 2011. Catalytic study on TiO_2 photocatalyst synthesised via microemulsion method on atrazine. *Sains Malaysiana* 40(8): 897- 902.

Teh, C.M. & Mohamed, A.R. 2011. Roles of titanium and ion-doped titanium dioxide on photocatalytic degradation of organic pollutants (phenolic compounds and dyes) in aqueous solutions: A review. *Journal of Alloy Compound* 509: 1648-1660.

Wan, F.K., Ho, L.N., Ong, S.A., Wong, Y.S., Nik, A.Y. & Fahmi, R. 2015. Decolorization and mineralization of Batik wastewater through solar photocatalytic process. *Sains Malaysiana* 44(4): 607-612.

Zhang, X., Wang, Y., You, Y., Meng, H., Zhang, J. & Xu, X. 2012. Preparation, performance and adsorption activity of TiO_2 nanoparticles entrapped PVDF hybrid membranes. *Applied Surface Science* 261: 660-665.

Zhu, T., Lin, Y., Hu, X., Lin, W., Yu, P. & Huang, C. 2012. Preparation and characterization of TiO_2-regenerated cellulose inorganic-polymer hybrid membranes for dehydration of caprolactam. *Carbohydrate Polymers* 87: 901-909.

Evyan Yang Chia Yan, Sarani Zakaria* & Chin Hua Chia
Bioresources and Biorefinery Laboratory,
School of Applied Physics
Faculty of Science and Technology
Universiti Kebangsaan Malaysia
43600 UKM Bangi, Selangor Darul Ehsan
Malaysia

Evyan Yang Chia Yan
Department of Applied Sciences
Faculty of Science and Technology
Nilai University, 1, Persiaran Universiti
71800 Nilai, Negeri Sembilan Darul Khusus
Malaysia

Thomas Rosenau
Division of Chemistry of Renewable Resource
Muthgasse 18, A-1190 Wien, Universität für Bodenkultur Wien
University of Natural Resources and Life Science, Vienn
Austria

*Corresponding author; email: szakaria@ukm.edu.my

Received: 20 April 2016
Accepted: 20 September 2016